



# Qualitative and Quantitative Evaluation of Morpho-Metabolic Changes in Bone Cartilage Complex of Knee Joint in Osteoarthritis Using Simultaneous $^{18}\text{F}$ -NaF PET/MRI—A Pilot Study

Amarnath Jena<sup>1</sup> Nidhi Goyal<sup>2</sup> Prerana Rana<sup>1,3</sup> Sangeeta Taneja<sup>1</sup> Abhishek Vaish<sup>4</sup> Rajesh Botchu<sup>5</sup>  
Raju Vaishya<sup>4</sup>

<sup>1</sup>Department of Molecular Imaging and Nuclear Medicine, Indraprastha Apollo Hospital, New Delhi, India

<sup>2</sup>Department of Radiodiagnosis and Imaging, Indraprastha Apollo Hospitals, New Delhi, India

<sup>3</sup>Apollo Hospitals Education and Research Foundation, Indraprastha Apollo Hospitals, New Delhi, India

<sup>4</sup>Department of Orthopaedics and Joint Replacement Surgery, Indraprastha Apollo Hospitals, New Delhi, India

<sup>5</sup>Department of Musculoskeletal Radiology, Royal Orthopedic Hospital, Birmingham, United Kingdom

Address for correspondence Rajesh Botchu, MBBS, MS (Ortho), MRCEd, MRCSI, FRCR, Department of Musculoskeletal Radiology, Royal Orthopedic Hospital, Birmingham B31 2AP, United Kingdom (e-mail: drbrajesh@yahoo.com).

Indian J Radiol Imaging 2023;33:173–182.

## Abstract

**Background** Articular cartilage (AC) loss and deterioration, as well as bone remodeling, are all symptoms of osteoarthritis (OA). As a result, an ideal imaging technique for researching OA is required, which must be sensitive to both soft tissue and bone health.

**Objective** The aim of this study was to assess the potential of simultaneous  $^{18}\text{F}$  sodium fluoride ( $^{18}\text{F}$ -NaF) positron emission tomography/magnetic resonance imaging (PET/MRI) to identify as well as classify osseous metabolic abnormalities in knee OA and to see if degenerative changes in the cartilage and bone on MRI might be correlated with subchondral  $^{18}\text{F}$ -NaF uptake on PET.

**Methods** Sixteen (32 knees) volunteers with no past history of knee injury, with or without pain, were enrolled for the research from January to July 2021. The images of both knees were taken utilizing an molecular magnetic resonance (mMR) body matrix coil on a simultaneous PET/MRI biograph mMR. The acquisition was conducted after 45 minutes of intravenous infusion of  $^{18}\text{F}$ -NaF 185–370 MBq (5–10 mCi) over one PET bed for 40 minutes, while MRI sequences were performed simultaneously.

**Results** All pathologies showed significantly higher maximum standardized uptake value ( $\text{SUV}_{\text{max}}$ ) than the background. Thirty-four subchondral magic spots were identified on  $^{18}\text{F}$ -NaF PET without any structural alteration on MRI. Bone marrow lesions (BMLs) and osteophytes with higher MRI osteoarthritis knee score (MOAKS) score showed higher  $^{18}\text{F}$ -NaF uptake ( $\text{grade}1 < \text{grade}2 < \text{grade}3$ ). BMLs had corresponding AC degeneration. There was discordance between grade 1 osteophytes (86.6%),

## Keywords

- ▶ osteoarthritis
- ▶ knee joints
- ▶ simultaneous PET/MRI
- ▶ cartilage
- ▶ bone

article published online  
January 6, 2023

DOI <https://doi.org/10.1055/s-0042-1760285>.  
ISSN 0971-3026.

© 2023. Indian Radiological Association. All rights reserved.  
This is an open access article published by Thieme under the terms of the Creative Commons Attribution-NonDerivative-NonCommercial-License, permitting copying and reproduction so long as the original work is given appropriate credit. Contents may not be used for commercial purposes, or adapted, remixed, transformed or built upon. (<https://creativecommons.org/licenses/by-nc-nd/4.0/>)  
Thieme Medical and Scientific Publishers Pvt. Ltd., A-12, 2nd Floor, Sector 2, Noida-201301 UP, India

sclerosis (53.7%) and grade 1 BML in cruciate ligament insertion site (91.66%); they did not have high uptake of 18F-NaF. In case of cartilage, there was significant difference between AC grades and average subchondral SUV<sub>max</sub> and T2\* relaxometry (grade0<grade1<grade2<grade3<grade4). BMLs are much more metabolically active than other pathologies, while sclerosis is the least. We also found that the subchondral uptake was statistically increased in the areas of pathology:

**Conclusion** 18F-NaF PET/MRI was able to detect knee abnormalities unseen on MRI alone and simultaneously assessed metabolic and structural markers of knee OA across multiple tissues in the joint. Thus, it is a promising tool for detection of early metabolic changes in OA.

## Introduction

Osteoarthritis (OA) is a commonly encountered degenerative joint disease, characterized by hypertrophic alterations in the bone, synovial inflammation, subchondral sclerosis, and joint space narrowing (JSN).<sup>1</sup> About 18.0% of women and 9.6% of men that are over the age of 60 have symptomatic OA based on global estimates. In terms of total years lost to disability, OA is the fifth most common cause in high-income nations and the ninth most common cause in low- and middle-income countries.<sup>2</sup> Since the current diagnostic modalities are inefficient to identify early development of OA, there are no proven and effective disease-modifying osteoarthritis drug (DMOAD) available.<sup>3</sup>

Magnetic resonance imaging (MRI) has demonstrated to be a promising imaging modality for OA research because it can measure pathology at the molecular level that radiography cannot see because biochemical alterations in the cartilage appear before morphologic abnormalities. Furthermore, MRI's advantages such as semiquantitative MRI, quantitative MRI, cartilage relaxometry, delayed gadolinium-enhanced MRI of cartilage, sodium MRI, glycosaminoglycan (GAG) chemical exchange saturation transfer (*gagCEST*), and others allow for a full OA workup and the modulation of multiple scan protocols to fit in with the research purpose.<sup>4-8</sup> A plausible explanation for the onset and progression of knee OA, a disorder characterized by the deterioration and loss of soft tissues such as cartilage, as well as the development of bone marrow lesions (BML) and osteophytes, is abnormal bone physiology.<sup>9</sup> The biochemical alterations inside the cartilage extracellular matrix (ECM) can be discovered using compositional MRI techniques such as T<sub>2</sub>, T<sub>2</sub>\*, or T1ρ but mostly focused on soft tissue.<sup>5</sup> Bone metabolism, on the other hand, cannot be accessed directly using MRI. Alterations in bone metabolism are recognized to arise with OA, especially in the subchondral region, recently it gained the attention of the researchers. Subchondral bone, despite many soft tissues in the joint, is a highly vascularized as well as metabolically active tissue that is constantly changing. Bone remodeling is used to adapt bone architecture to changing mechanical pressures on joints, restore microdamage in the bone matrix, and react to trauma or bone pathology. While optimal joint function depends on subchondral

bone remodeling, greater bone remodeling has been associated to the progression of OA, especially in the initial stages of the illness.<sup>10</sup>

Since 1972, the 18F sodium fluoride (18F-NaF) radiotracer has been used to noninvasively examine regional subchondral bone features and bony remodeling. 18F-NaF absorption is concentrated in newly mineralizing bone sites and is employed as a bone metabolism marker.<sup>11,12</sup>

As above mentioned, articular cartilage loss and deterioration, as well as bone remodeling, are all symptoms of OA. As a result, an ideal imaging technique for researching OA is required, which must be sensitive to both soft tissue and bone health. While MRI is unparalleled in terms of assessing bone marrow disease and soft tissue, functional bone imaging is still a hurdle. PET has a one-of-a-kind ability to provide quantitative data on molecular and physiological activity, which can often predict structural and biochemical alterations, but it requires the assistance of higher-resolution anatomic data to locate these physiologic events. This opens up the possibility of assessing the function of metabolic activity in OA using positron emission tomography (PET) markers while also relating them to qualitative MRI measures of OA bone diseases.<sup>13</sup>

The aim of our study was to assess the potential of simultaneous 18F-NaF PET/MRI to identify as well as classify osseous metabolic abnormalities in knee OA and to see if degenerative changes in the cartilage and bone on MRI might be correlated with subchondral 18F-NaF uptake on PET.

## Material and Methods

### Study Population

Sixteen (32 knees) volunteers with no past history of knee injury, with or without pain, were enrolled for the research from January to July 2021. Preliminary to the trial, radiographs were obtained, and musculoskeletal radiologists with over 15 years of expertise graded the radiographs using Kellgren and Lawrence (KL) grading.<sup>14</sup> Based on KL grading, the patients were segregated into three study groups: (1) subjects without pain with KL grade 0 (13 knees); (2) subjects without pain with KL score >0 (6 knees); and (3) subjects with pain with KL grade >0 (13 knees) (► **Table 1**). Pregnant and breast-feeding

**Table 1** Study demography

Total no. of patients	16 (32 knees)
Mean age	41 ± 11.83 years (30–63 years)
Male	9
Female	7
BMI	24.4 ± 3.6 kg/m <sup>2</sup>
Study group	
Subjects without pain with KL grade 0 (group 1)	13 knees
Subjects without pain with KL score >0 (group 2)	6 knees
Subjects with pain with KL grade >0 (group 3)	11 knees

Abbreviations: BMI, body mass Index; KL, Kellgren and Lawrence.

women, patients taking an investigational drug, age less than 30 years; patients who had knee fracture or surgical intervention, history of diseases involving the studied joint such as Paget's disease, systemic inflammatory diseases, avascular necrosis, crystalline diseases or tumors; and patients who were claustrophobic and had MRI contraindicated are all excluded from study. This study did not include any cases of related co-morbid inflammatory arthritis. All of the patients' histories corroborated this. All participants were notified about the study's purpose before being asked to participate, and written consent was acquired. The Institutional Review Board (IAH-BMR-027/08–20) approved this prospective study and it was Human Research Protection Program–compliant.

### PET-MRI Scanning

The images of both knees were taken utilizing an molecular magnetic resonance (mMR) body matrix coil on a simultaneous PET/MRI Biograph mMR (Siemens, Erlangen, Germany). The acquisition was conducted after 45 minutes of intravenous infusion of 18F-NaF 185–370 MBq (5–10 mCi) over one PET bed (field of view = 26 cm, matrix 172 × 172) for 40 minutes, while MRI sequences were performed simultaneously (MRI sequences was enlisted in ► **Table 2**). Following the scan, all coincident data were sorted into a two-dimensional-PET sinogram, which was subsequently reconstructed into transaxial sections, with an iterative 3D-ordered-subset expectation maximization algorithm with 3 iterations and 21 subsets, Gaussian smoothing of 6 mm full width at half maximum, and a zoom of 1. Dixon-based MR-based attenuation correction images were used for attenuation correction and the attenuation maps for PET/MRI were generated from them. The three-dimensional sequence with iPAT technology also offers the benefit of high-resolution isotropic imaging, which helps to reduce the partial volume effect between cartilage and synovial fluid. MRI, PET, and PET/MR imaging scans were reviewed at syngo platform (Siemens, Erlangen, Germany).

**Table 2** MRI parameters

Acquisition parameters	MRI sequences									
	T1WI (AC sequence)	3D MEDIC	Sagittal T2 SPAIR	Coronal T2 SPAIR	T1 TSE	Sagittal T2* MAP	Coronal T2* MAP	Axial T2* MAP		
TR (ms)	3.6	38	8540	6790	433	1120	1120	1120		
TE (ms)	2.5, 1.2	16	50	60	11	4.36, 11.90, 19.44, 26.98	4.36, 11.90, 19.44, 26.98	4.36, 11.90, 19.44, 26.98		
TA (min)	0.19	5.24	3.18	2.24	2.03	3.07	4.05	3.07		
FA (degree)	10	8	120	120	120	60	60	60		
Voxel size (mm)	4.1 × 2.6 × 3.1	0.6 × 0.5 × 0.9	0.5 × 0.4 × 3.5	0.5 × 0.4 × 3.5	0.6 × 0.36 × 3.5	0.5 × 0.4 × 3.5	0.5 × 0.4 × 3.5	0.5 × 0.4 × 3.5		
Slice thickness	3.2	0.9	3.5	3.5	3.5	3.5	3.5	3.5		
No. of slices	128	128	28	23	28	28	28	28		
FOV	500	140	140	140	140	140	140	140		
Matrix size (mm)	192 × 192	256 × 256	384 × 384	384 × 384	384 × 384	320 × 320	320 × 320	320 × 320		
iPATZ	yes	yes	no	yes	no	yes	yes	yes		

Abbreviations: AC, attenuation correction; FOV, field of view; mm, millimeter; MAP, mean arterial pressure; MRI, magnetic resonance imaging; SPAIR, spectral attenuated inversion recovery; TA, time of acquisition; TE, time to echo; TR, time to repeat; TSE, turbo spin echo.

### 18F-NaF Dosimetry

18F-NaF is a positron emitter; positron itself (mean energy, 250 keV) and by the two 511-keV annihilation photons delivers the energy.<sup>15</sup> Almost all of the kinetic energy of the 18F-NaF positron will be deposited in the source organ. 0.024 mSv/MBq (0.089 mrem/mCi) is the effective dose for 18F. The effective dose for a typical activity of 370 MBq (10 mCi) is 8.9 mSv (0.89 rem). The bladder obtained highest radiation dose, that is, receiving 0.22 mGy/MBq (0.81 rad/mCi) for 185–370 MBq (5–10 mCi) activity.<sup>16</sup>

### Image Analysis

Images were analyzed by two trained musculoskeletal radiologists and two nuclear medicine physicians with more than 15 years of experience. They identified BMLs as areas of high T2 signal in subchondral bone, osteophytes identified as bony protrusions on T1 turbo spin echo (TSE) images, articular cartilage was evaluated on T2 spectral attenuated inversion recovery sequence and subchondral sclerosis, identified as subchondral bone with low signal intensity on both fat saturated T2-weighted images and T1 TSE images and corresponding uptake of 18F-NaF on PET image. The BMLs (grade 0 = none, grade 1 <33%, grade 2 = 33–66%, and grade 3 >66%) and osteophytes (grade 0 = none; grade 1 = small; grade 2 = medium; grade 3 = large) were scored using MRI osteoarthritis knee score (MOAKS) criteria.<sup>17</sup> For 18F-NaF study, volume of interests (VOIs) with SUV greater than 3 times the reference SUV (background SUV) in normal bone (i.e., SUV from a region of normal-appearing trabecular bone/ the medial femoral condyle) was identified as high uptake VOI (VOI<sub>High</sub>) on PET SUV maps, i.e., PET positive. All high maximum standardized uptake value SUV (SUV<sub>max</sub>) VOIs was assessed with corresponding MRI regions for presence of any anatomical correlates. Also abnormal anatomical regions [region of interest (ROI)] were assessed for PET correlation by adopting copy paste technique. The high uptake VOI's without any structural change was termed as "Subchondral magic spot." Cartilage was graded according to an MRI-modified Outerbridge classification (grade 0: cartilage that appears normal; grade 1: focal hyperintense regions inside a normal contour; grade 2: Surface-extending articular cartilage fissure or blister-like swelling; grade 3: "Crab meat" lesions and localized ulcerations; grade 4: full-thickness cartilage loss with underlying bone reactive changes).<sup>18</sup> Each knee was divided into 8 compartments, i.e., patella, trochlea (Troc), medial central femur (MCF), lateral central femur (LCF), medial posterior femur (MPF), lateral posterior femur (LPF), medial tibia (MT), lateral tibia (LT) which was further divided as: patella - medial patella and lateral patella, Troc-medial trochlea and lateral trochlea, MCF, LCF, MPF, LPF, MT- medial anterior tibia, medial central tibia, medial posterior tibia, LT - lateral anterior tibia, lateral central tibia, lateral posterior tibia. For BML evaluation, we also take into consideration the cruciate ligament (CL) insertion sites as per MOAKS criteria.

SUV<sub>max</sub> on PET images in different bone pathologies (identified on MRI) as well as from normal-appearing bone, PET uptake related to BML, and osteophyte grades identified on MRI and differences in 18F-NaF PET uptake

for different adjacent cartilage grades determined from MR images were analyzed using ANOVA.

### Statistical Analyses

All statistical analyses were performed using the MedCalc statistical software package (version 19.8- 64 bit; Windows Vista/7/8/10) and *p*-Values less than 0.05 were considered statistically significant.

### Results

Subchondral bone and cartilage features of OA were identified on MRI in all. In the 32 knee joints analyzed in our study, 53 BMLs [42-grade 1 (79.2%); 9-grade 2 (16.9%); 2-grade 3 (3.7%)], 177 osteophytes [150-grade 1 (84.7%); 13-grade 2 (7.3%), 14-grade 3 (7.9%)], and 54 areas of subchondral sclerosis were identified on MRI and graded using a MOAKS classification. Additionally, 34 subchondral magic spots were identified on 18F-NaF PET. MRI grading of cartilage revealed 309 areas of normal appearing cartilage (grade 0), 121 areas of mild degeneration (grades 1–2), and 18 areas of severe degeneration (grade 3–4) (total regions 452) (► **Fig. 1A and B**).

BMLs with higher MOAKS score on MRI showed higher 18F-NaF uptake on PET. Mean SUV<sub>max</sub> of  $2.7 \pm 2.3$ ,  $9.5 \pm 3.8$ , and  $48.5 \pm 8.8$  were observed in grade 1, grade 2, and grade 3, BMLs, respectively. Statistically significantly higher SUV<sub>max</sub> was noted in grade 2 and grade 3 BMLs than grade 1 BMLs ( $p < 0.001$  for both). Grade 3 showed greater uptake than grade 2 BMLs ( $p = 0.00$ ). The pattern that was observed: grade 1 < grade 2 < grade 3 (► **Supplementary Fig. S1**, available in the online version only). All grade 2 (9 of 9 [100%]) and grade 3 (2 of 2 [100%]) BMLs identified on MRI corresponded to VOI<sub>High</sub> identified on 18F-NaF PET, and the concordance in grade 1 BMLs in bony compartments was also high (15 of 18 [88.8%]), but grade 1 BML in CL insertion site shows low level of concordance (2 of 24 [9.09%]). BMLs had corresponding AC cartilage degeneration, that is, grade 1 BML in bony compartments had 4 grade 1, 11 grade 2, 1 grade 3, and 1 grade 4 associated AC cartilage degeneration, whereas only 1 BML did not show any association; grade 2 BML had 4 grade 2, 1 grade 3, and 3 grade 4 associated AC cartilage degeneration, whereas only 1 BML did not show any association; and grade 3 BML had 1 grade 3 and 1 grade 4 associated AC cartilage degeneration. That means 93.1% (27 out of 29 BMLs in bony compartment) BMLs had associated adjacent cartilage degeneration.

Osteophytes with higher MOAKS score on MRI showed higher 18F-NaF uptake on PET. Mean SUV<sub>max</sub> of  $1.3 \pm 0.8$ ,  $4.05 \pm 1.8$ , and  $6.64 \pm 2.7$  were observed in grade 1, grade 2, and grade 3 osteophytes, respectively. Grade 2 and 3 osteophytes also showed statistically significantly higher SUV<sub>max</sub> than grade 1 osteophytes ( $p < 0.00$  for both) and between grade 2 and grade 3 the difference was statistically significant, that is, *p*-value was 0.008. The pattern that was observed—grade 1 < grade 2 < grade 3 (► **Supplementary Fig. S2**, available in the online version only). While concordance with VOI<sub>High</sub> on 18F-NaF PET was observed between all grade 2 (13 of 13 [100%]) and all grade 3 (14 of 14 [100%]) osteophytes identified on MRI, but lower number (40 of 150

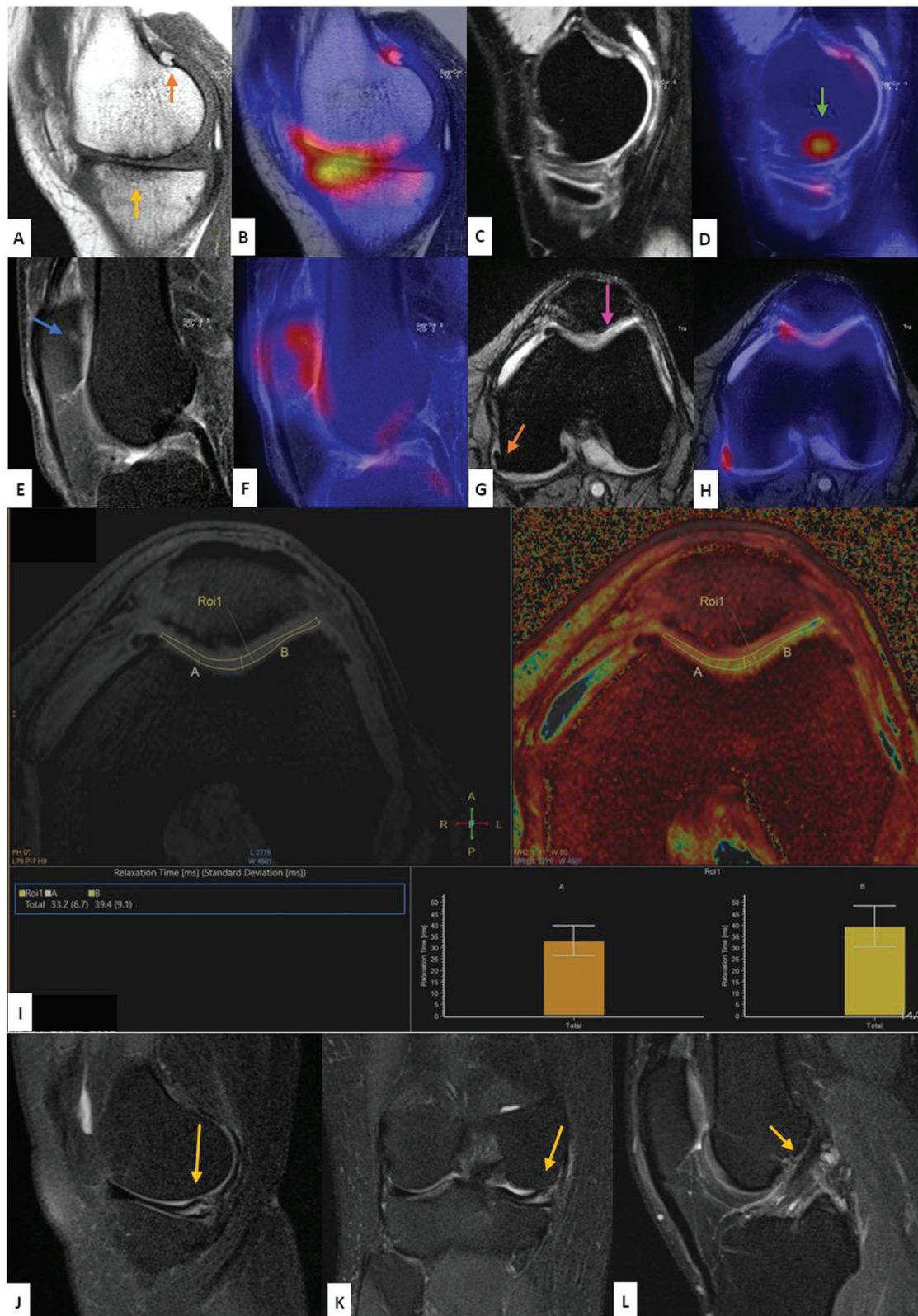


**Fig. 1** <sup>18</sup>F sodium fluoride (<sup>18</sup>F-NaF) served as a one-stop modality to assess whole joint, that is, bone pathology, cartilage, and ligaments (sagittal T1 turbo spin echo) showed osteophyte (orange arrow) and sclerosis (yellow arrow) with corresponding <sup>18</sup>F-NaF uptake (B; fused positron emission tomography/magnetic resonance imaging [PET/MRI]); (C) sagittal three-dimensional MEDIC did not have any structural abnormality but when fused with PET (D) there was high uptake volume of interest (green arrow) termed as “subchondral magic spot”; (E) sagittal T2 spectral attenuated inversion recovery [SPAIR]) depicted grade 1 BML (blue arrow) with corresponding uptake in fused PET/MRI (F) G (axial T2\*) showed degenerated medial and lateral trochlear cartilage (pink arrow) with corresponding fused PET/MRI (H) and T2\* relaxometry (I) that raised values. Additional findings that can be obtained with PET/MRI scan. J (sagittal T2 SPAIR) and K (coronal T2 SPAIR) showed medial meniscal tear and image L (sagittal T2 SPAIR) showed mucoid degeneration of anterior cruciate ligament.

[13.3%]) of the grade 1 osteophytes identified on MRI corresponded to VOI<sub>High</sub> on 18F-NaF PET. Grade 1 osteophytes had 38 grade 1, 8 grade 2, and 3 grade 3 associated AC cartilage degeneration, whereas 101 osteophytes did not show any association; grade 2 osteophytes had 2 grade 1, 6 grade 2, 3 grade 3, and 1 grade 4 associated AC cartilage degeneration, whereas only 1 osteophytes did not show any association; and grade 3 osteophytes had 3 grade 1, 4 grade 2, 3 grade 3, and 4 grade 4 associated AC cartilage degeneration. That means 42.3% (102 out of 177) osteophytes had associated adjacent cartilage degeneration.

The sclerosis showed high SUV<sub>max</sub> value  $1.94 \pm 1.45$  that was statistically significantly higher than the background values, that is,  $0.63 \pm 0.35$  ( $p = 0.000$ ). There were only two regions containing sclerosis, that is, MT and LT with average SUV<sub>max</sub>  $2.06 \pm 1.7$  and  $1.73 \pm 0.72$ , respectively. Fewer than half 25 of 54 [100%]) of sclerotic areas identified on MRI corresponded to VOI<sub>High</sub> identified on 18F-NaF PET. Also, only 4 out of 54 (7.4%) sclerotic regions had associated cartilage degeneration. The subchondral magic spot showed high SUV<sub>max</sub> value  $2.52 \pm 1.17$  that was statistically significantly higher than the background values, that is,  $0.64 \pm 0.41$  ( $p = 0.000$ ). Also, only 2 out of 34 (5.8%) magic spot regions had associated cartilage degeneration. There was statistically significant difference between SUV<sub>max</sub> among different OA pathologies ( $p < 0.000$ ), that is, the pattern of SUV<sub>max</sub>: BML > osteophyte > subchondral magic spot > sclerosis (→ **Supplementary Fig. S3**, available in the online version only).

In case of cartilage, there was significant difference between average SUV<sub>max</sub> between the AC cartilage grades, that is,  $p$ -value = 0.000. The pattern that we observed in case of SUV<sub>max</sub> was grade 0 < grade 1 < grade 2 < grade 3 < grade 4 (→ **Table 3** and → **Fig. 2**).

On analysis of T2\* relaxometry with respect to AC grade, we found statistically significant difference between average T2\* values between the AC cartilage grade. The pattern that we observed in case of T2\* values was grade 0 < grade 1 < grade 2 < grade 3 < grade 4 (→ **Table 4** and → **Fig. 3**).

We found that the subchondral uptake was statistically increased in the areas of pathology:

**Osteophyte:** The areas without osteophyte had average SUV<sub>max</sub> value  $1.51 \pm 1.21$  and areas containing osteophytes had  $1.98 \pm 1.8$  ( $p$ -value = 0.000).

**Table 3** SUV<sub>max</sub> and number of areas with respect to AC grade

AC grade	No. of areas	SUV <sub>max</sub>
0	309	$1.09 \pm 0.62$
1	76	$1.31 \pm 0.7$
2	45	$2.11 \pm 1.3$
3	10	$3.27 \pm 1.7$
4	8	$5.72 \pm 1.3$

Abbreviations: AC, articular cartilage; SUV<sub>max</sub>, maximum standard uptake value.

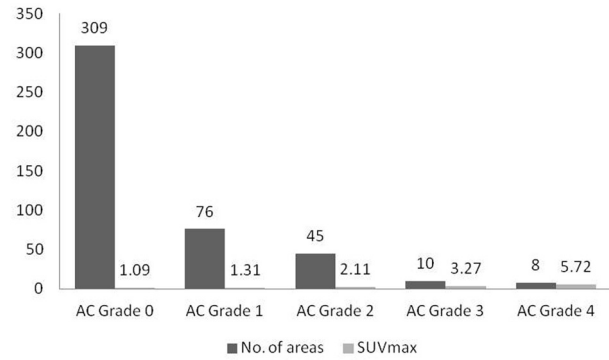


**Fig. 2** Maximum standard uptake value (SUV<sub>max</sub>) and number of areas with respect to articular cartilage (AC) grade.

**Table 4** T2\* relaxometry value and number of areas with respect to AC grade

AC grade	No. of areas	SUV <sub>max</sub>
0	309	$25.2 \pm 4.7$
1	76	$31.3 \pm 5.1$
2	45	$32.5 \pm 5.3$
3	10	$38.9 \pm 6.4$
4	8	$46 \pm 17.5$

Abbreviations: AC, articular cartilage; SUV<sub>max</sub>, maximum standard uptake value.

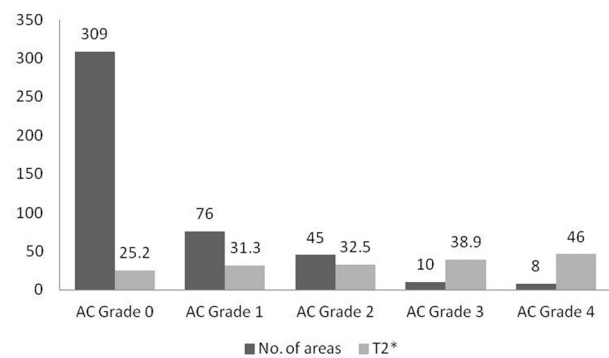


**Fig. 3** T2\* relaxometry value and number of areas with respect to articular cartilage (AC) grade.

**BMLs:** The areas without BMLs had average SUV<sub>max</sub> value  $3.6 \pm 1.9$  and areas containing BMLs had  $10 \pm 11.9$  ( $p$ -value = 0.008).

**Sclerosis:** The areas without sclerosis had average SUV<sub>max</sub> value  $1.5 \pm 1.3$  and areas containing sclerosis had  $1.89 \pm 1.4$  ( $p$ -value = 0.001).

**Subchondral magic spots** the areas without this uptake had average SUV<sub>max</sub> value  $1.4 \pm 0.6$  and areas containing this had  $2.2 \pm 0.9$  ( $p$ -value = 0.000).

## Discussion

This is an observational study, which aimed to uniquely assess metabolic and structural markers of knee OA simultaneously across multiple tissues in the joint. Hybrid PET-MR

scanners enable for quantitative, sensitive, and simultaneous evaluation of articular cartilage, other soft tissues, and bone; thus they could be the most effective way to research OA. For the examination of joints and soft tissue, MRI became the gold standard. This study demonstrates that the incorporation of PET allows for the simultaneous estimation of variations in metabolic activity of bone that will not only aid in the understanding of OA bone pathology, but it could also offer vital evidence on the linkage of bone remodeling with soft tissue changes. On the molecular level, PET imaging offers for a quantitative evaluation of functional alterations in OA. While bone pathology has traditionally been assumed to play a significant role in the evolution of OA, the etiology, activity, as well as progression of the disease is still unknown.<sup>13,19</sup> The susceptibility of 18F-NaF PET to osteoblastic activities was exhibited in this investigation, as well as its ability to quantify remodeling of subchondral bone and also other metabolic anomalies in OA bone pathology.

Observations of alterations that were only visible on PET as areas of elevated 18F-NaF uptake, that is, “subchondral magic spot” are particularly intriguing. 18F-NaF could serve as a biomarker of early bone remodeling alterations that arise prior to structural MRI degradation that is evident in the joint, because molecular alterations typically herald tissue level variations. In a study by Kogan et al, they also noticed these areas that are termed as VOI<sub>high</sub> without any structural changes on corresponding MRI in their study, which they labeled as early OA markers and also reported a linkage with adjacent mild (grade 1–2) cartilage degeneration, but we did not find this association in our study.<sup>20</sup> Only 2 out of 34 magic spot regions (VOI<sub>high</sub> areas) were associated with adjacent mild cartilage degeneration. The osteoblast activity seen on 18F-NaF is an excellent option for biomarkers that can efficiently assess early OA initiation and progression, which is critical for the development as well as assessment of DMOAD.

An absence of metabolic activity could also imply that some pathology served a scanty role in the active progression of OA. There was discordance between grade 1 osteophytes (86.6%), sclerosis (53.7%), and grade 1 BML in CL insertion site (91.66%) identified on MRI; they did not have high uptake of 18F-NaF PET. Grade 1 osteophytes were found to be discordant in Kogan et al investigation, but grade 1 BML in the CL insertion site and sclerosis is a new observation.<sup>20</sup> The initial symptoms of radiographic OA are assumed to be these tiny osteophytes, and PET data suggests that their metabolic activity is not enhanced. 18F-NaF PET can be used to identify these lesions and investigate their impact on the course of OA.

According to our findings, BMLs were much more metabolically active than other pathologies, while sclerosis was the least metabolically active. Moreover, BMLs and osteophytes of higher grade detected on MRI showed higher uptake of 18 F-fluoride. However, among each type of bone abnormality as well as within each lesion grade, there were considerable standard deviation. These findings were in line with the study of Kogan et al. The 18F-NaF PET's sensitivity to bone remodeling may allow us to adequately

comprehend and describe individual subchondral bone lesions.

BMLs are regarded as important drivers of pain and are associated with the radiographic severity of OA and elevated incidence of OA progression; they have been a focus of increasing attention in OA.<sup>21–23</sup> While there is a possible link between BMLs and OA symptoms, current BML detection as areas of elevated signal in bone on fat suppressed T2w images is not quantifiable and is frequently a late finding. As a result, the impact of individual MRI-identified lesions on the course of OA remains unclear. 18F-NaF PET in BMLs can be used to measure osteoblast metabolic activity and bone remodeling. Our 18F-NaF data showed that BMLs found on MRI are much more metabolically active for bone remodeling than other bone pathologies (such as osteophytes and sclerosis) and normal-appearing sites on MRI. In comparison to other bone pathologies as seen in results, BMLs were associated with more cartilage deterioration, that is, 93.1% of BMLs were associated with adjacent cartilage degeneration as compared with 42.3% in osteophytes, 7.4% in sclerosis and 5.85% in magic spot regions. The discovery of a relationship between BMLs and cartilage deterioration is consistent with previous research that related BMLs to the loss and degeneration of the surrounding cartilage.<sup>24,25</sup>

Subchondral bone uptake was significantly higher adjacent to severely (grade 3–4) degenerated cartilage than adjacent to mildly (grade 1–2) degenerated and normal cartilage. However, within each group, there were considerable standard deviation. In their investigation, Kogan et al discovered the same pattern of subchondral bone uptake near cartilage degradation.<sup>20</sup> We also discovered that the presence of bony pathologies increased the 18F-Fluoride uptake in subchondral bone (BML, osteophytes, VOI high, sclerosis).

T2\* relaxometry value of the severely (grade 3–4) degenerated cartilage was statistically higher than mildly (grade 1–2) degenerated and normal cartilage and standard deviation within each group was also high. In the instance of T2\* relaxometry, our findings are consistent with Lee et al findings; in their study also they also found that larger T2\* values corresponded to increased cartilage degradation in a canine model.<sup>26</sup> However, in a research by Mankin et al, T2\* values declined as cartilage deterioration progressed.<sup>27</sup>

Even though the cause of these findings is unknown, it may be possible due to signal averaging, in which the effects of cartilage matrix degradation that promote T2\* decay are counteracted by including fluid, such as an increase in cartilage water content or the inclusion of extracellular fluid in cartilage fissures, in the T2\* relaxation calculation. Even if bulk T2\* measurements rise with early cartilage degradation, the T2\* response to cartilage degeneration is multifactorially conditioned, diverse, and most likely nonlinear.<sup>27–29</sup>

T2\* mapping despite all the enumerated advantages, and its contribution to enhancing cartilage status assessment, is still evolving. T2\* mapping values are determined by several factors, such as the cartilage biochemical state, physics parameters used in the mapping, and the patient's physiology.<sup>30</sup>

**Table 5** Radiopharmaceuticals List

Radiopharmaceutical	Radionuclide	Target
18F-Fluoride	18F	Bone flow and bone remodeling
18F-FDG		Glucose metabolism, inflammation
[18F]DPA-714		Monocytes and macrophages (binds to peripheral benzodiazepine receptors)
[18F]fluoro-PEG-folate		Activated macrophages, folate receptor
[11C]-Choline	11C	Cell membrane synthesis, inflammation
[11C]PBR28		Monocytes and macrophages (binds to peripheral benzodiazepine receptors)
[11C]DPA-713		
[11C]PK11195		
[124I]-rituximab	124I	B cells
68Ga-labeled Siglec-9 peptide	68Ga	Inflammation
[68Ga]-PRGD2		Angiogenesis, targets Vb3 integrin

One of the most significant advantages of imaging of OA by using hybrid PET-MR is the capacity to assess morphologic and molecular spatial correlations among various tissues at the same time. The link among morphology of cartilage and subchondral bone pathology metabolic bony activity was investigated in this study. A trend was seen between increased 18F-NaF PET uptakes and increasing structural degeneration in the adjacent cartilage as semiquantitatively assessed using a modified Outerbridge scoring system. This finding suggests that degenerative changes and processes in bone and cartilage are linked. 18F-NaF PET, in combination with early MRI metrics of cartilage biochemistry, may provide an optimal method to study relationships between adjacent tissue degeneration in early OA.

Apart from the fact that a PET/MRI scan is a time-consuming and expensive process, there are certain other limitations to this study. First, no histopathology was acquired; thus we could not confirm that high PET uptake correlated to bone pathology. Instead, we have described these as abnormalities in bone metabolism. Second, the patient population in this study was smaller and heterogeneous including a range of ages. As a feasibility study, we felt it appropriate to study a broad range of subjects. Third, while an association between 18F-NaF uptake in subchondral bone and cartilage damage on MRI was observed, longitudinal studies are needed to determine the chronological order of these changes. Fourth, we believe the BMLs in these subjects are the result of degenerative osteoarthropathy, but serial tracking of these lesions is needed to better understand the role of bone remodeling and inflammation in these pathologies, as BMLs are heterogeneous with a diverse etiology and their size and features are known to change over time. Lastly, due to MR-based attenuation correction of its PET images, PET/MR is also known to underestimate SUV values by approximately 10%.<sup>31</sup>

18F-FDG, can also be employed in OA imaging, exhibits glucose metabolism and sensitivity to acute-phase cellular response regions (neutrophils or polymorphonuclear leukocytes), like inflammation. It had been shown that subchon-

dral bone marrow, periarticular, and intercondylar notch regions matching to BMLs detected on MRI exhibit increased FDG uptake in knee OA. Other tracers can also be used for OA in addition to these two radiotracers because of the pathogenesis of OA, which includes changes in synthetic activity and degradation; cell proliferation and cell death (apoptosis); the formation of new blood vessels; inflammation; and the activation of macrophages, B cells, and T cells (► **Table 5**). The majority of other radiopharmaceuticals are primarily used to treat rheumatoid arthritis; however, due to the properties mentioned above, their use may soon be expanded to treat OA.<sup>32</sup> Also, over the past few years, personalised medicine has attracted a lot of attention and evolved to signify many different things to many parties involved. Improvements have been achieved in the assessment and qualification of OA-specific biomarkers over the past 15 years. Because of this, it is currently common practice to classify these OA-specific biomarkers using the BIPEDS classification, which is based on the following essential factors: burden of illness (B), investigative (I), prognostic (P), efficacy of intervention (E), diagnostic (D), and safety (S). Radiographically (X-ray) defined JSN is currently the only imaging end point advised by both the U.S. Food and Drug Administration (FDA) and the European Agency for the Evaluation of Medicinal Products (EMA) guidance documents for clinical studies of DMOADs. Nevertheless, the joint space consisted of cartilage and meniscal integrity, and JSN has inadequate sensitivity to detect structural alterations. Following the FDA's recent formal recognition of OA as a serious condition, the agency is willing to consider appropriate surrogate for primary outcomes in clinical trials evaluating DMOADs, such as imaging or biochemical markers linked to cartilage loss.<sup>33</sup> Therefore, we anticipate that in the near future, PET/MRI will be utilized to track the effectiveness of these newly developed DMOADs by combining quantitative and dynamic PET with a variety of MRI features, including sodium MRI, gagCEST, and Magnetization transfer contrast (MTC). The findings of this study are observations, which highlight the potential of PET/MRI to simultaneously



study multiple functional and morphologic factors in the knee. More targeted studies in homogeneous patient cohorts are needed to make conclusions about the use of <sup>18</sup>F-NaF or <sup>18</sup>F-FDG as markers of OA pathogenesis.

## Conclusion

We present a novel technique to simultaneously assess metabolic and structural markers of knee OA across multiple tissues in the joint. Simultaneous <sup>18</sup>F-NaF PET/MR is able to detect knee abnormalities unseen on MRI alone and is a promising tool for detection of early metabolic changes in OA. Further, higher <sup>18</sup>F-NaF uptake corresponds to worse degeneration in the adjacent cartilage, suggesting a spatial relationship between bone remodeling and cartilage health. PET/MR thus can simultaneously assess multiple early metabolic and biochemical markers of knee OA progression across all tissues in the joint. This information may provide new insights into OA pathogenesis and may lead to new treatment targets to arrest the onset and progression of OA.

### Funding

Apollo Hospital Educational Research Foundation (AHERF), Wallace, Gardens, Chennai, Tamil Nadu, is a not-for-profit foundation of India recognized by the Department of Scientific and Industrial Research (DSIR) as a Scientific and Industrial Research Organisation (SIRO). AHERF had funded this work under the Faculty Development Program (FDP).

### Conflict of Interest

None declared.

## References

- Azad CS, Singh AK, Pandey P, et al. Osteoarthritis in India: an epidemiologic aspect. *Int J Recent Sci Res* 2017;8(10):20918–20922
- World Health Organization. "Chronic Rheumatic Conditions." Chronic diseases and health promotion. 2012. Accessed December 17, 2022 at: <http://www.who.int/chp/topics/rheumatic/en/>
- Teitel AD, Zieve D. MedlinePlus Medical Encyclopedia. National Institutes of Health. "Osteoarthritis." Accessed December 17, 2022 at: <http://www.nlm.nih.gov/medlineplus/ency/article/000423.htm>
- Wirth W, Buck R, Nevitt M, et al; OAI Investigators. MRI-based extended ordered values more efficiently differentiate cartilage loss in knees with and without joint space narrowing than region-specific approaches using MRI or radiography—data from the OA initiative. *Osteoarthritis Cartilage* 2011;19(06):689–699
- Binks DA, Hodgson RJ, Ries ME, et al. Quantitative parametric MRI of articular cartilage: a review of progress and open challenges. *Br J Radiol* 2013;86(1023):20120163. Doi: 10.1259/bjr.20120163
- Williams A, Qian Y, Golla S, Chu CR. UTE-T2\* mapping detects sub-clinical meniscus injury after anterior cruciate ligament tear. *Osteoarthritis Cartilage* 2012;20(06):486–494
- Ling W, Regatte RR, Navon G, Jerschow A. Assessment of glycosaminoglycan concentration in vivo by chemical exchange-dependent saturation transfer (gagCEST). *Proc Natl Acad Sci USA* 2008;105(07):2266–2270
- Madelin G, Babb J, Xia D, et al. Articular cartilage: evaluation with fluid-suppressed 7.0-T sodium MR imaging in subjects with and subjects without osteoarthritis. *Radiology* 2013;268(02):481–491
- Watkins L, MacKay J, Haddock B, et al. Assessment of quantitative [<sup>18</sup>F]Sodium fluoride PET measures of knee subchondral bone perfusion and mineralization in osteoarthritic and healthy subjects. *Osteoarthritis Cartilage* 2021;29(06):849–858
- Burr DB, Gallant MA. Bone remodelling in osteoarthritis. *Nat Rev Rheumatol* 2012;8(11):665–673
- Blau M, Nagler W, Bender MA. Fluorine-18: a new isotope for bone scanning. *J Nucl Med* 1962;3:332–334
- Jadvar H, Desai B, Conti PS. Sodium <sup>18</sup>F-fluoride PET/CT of bone, joint, and other disorders. *Semin Nucl Med* 2015;45(01):58–65
- Kogan F, Broski SM, Yoon D, Gold GE. Applications of PET-MRI in musculoskeletal disease. *J Magn Reson Imaging* 2018;48(01):27–47
- Kohn MD, Sassoon AA, Fernando ND. Classifications in brief: Kellgren-Lawrence classification of osteoarthritis. *Clin Orthop Relat Res* 2016;474(08):1886–1893
- Grant FD, Fahey FH, Packard AB, Davis RT, Alavi A, Treves ST. Skeletal PET with <sup>18</sup>F-fluoride: applying new technology to an old tracer. *J Nucl Med* 2008;49(01):68–78
- Segall G, Delbeke D, Stabin MG, et al; SNM. SNM practice guideline for sodium <sup>18</sup>F-fluoride PET/CT bone scans 1.0. *J Nucl Med* 2010;51(11):1813–1820
- Hunter DJ, Guermazi A, Lo GH, et al. Evolution of semi-quantitative whole joint assessment of knee OA: MOAKS (MRI Osteoarthritis Knee Score). *Osteoarthritis Cartilage* 2011;19(08):990–1002
- Paunipagar BK, Rasalkar D. Imaging of articular cartilage. *Indian J Radiol Imaging* 2014;24(03):237–248
- Torigian DA, Zaidi H, Kwee TC, et al. PET/MR imaging: technical aspects and potential clinical applications. *Radiology* 2013;267(01):26–44
- Kogan F, Fan AP, McWalter EJ, Oei EH, Quon A, Gold GE. PET/MRI of metabolic activity in osteoarthritis: a feasibility study. *J Magn Reson Imaging* 2017;45(06):1736–1745
- Felson DT, Chaisson CE, Hill CL, et al. The association of bone marrow lesions with pain in knee osteoarthritis. *Ann Intern Med* 2001;134(07):541–549
- Link TM, Steinbach LS, Ghosh S, et al. Osteoarthritis: MR imaging findings in different stages of disease and correlation with clinical findings. *Radiology* 2003;226(02):373–381
- Felson DT, McLaughlin S, Goggins J, et al. Bone marrow edema and its relation to progression of knee osteoarthritis. *Ann Intern Med* 2003;139(5 Pt 1):330–336
- Roemer FW, Guermazi A, Javard MK, et al; MOST Study investigators. Change in MRI-detected subchondral bone marrow lesions is associated with cartilage loss: the MOST study. A longitudinal multicentre study of knee osteoarthritis. *Ann Rheum Dis* 2009;68(09):1461–1465
- Muratovic D, Cicuttini F, Wluka A, et al. Bone marrow lesions detected by specific combination of MRI sequences are associated with severity of osteochondral degeneration. *Arthritis Res Ther* 2016;18:54
- Lee D, Hong KT, Lim TS, et al. Alterations in articular cartilage T2 star relaxation time following mechanical disorders: in vivo canine supraspinatus tendon resection models. *BMC Musculoskelet Disord* 2020;21(01):424
- Mankin HJ, Dorfman H, Lippiello L, Zarins A. Biochemical and metabolic abnormalities in articular cartilage from osteoarthritic human hips. II. Correlation of morphology with biochemical and metabolic data. *J Bone Joint Surg Am* 1971;53(03):523–537
- Williams A, Qian Y, Bear D, Chu CR. Assessing degeneration of human articular cartilage with ultra-short echo time (UTE) T2\* mapping. *Osteoarthritis Cartilage* 2010;18(04):539–546
- Guermazi A, Alizai H, Crema MD, Trattinig S, Regatte RR, Roemer FW. Compositional MRI techniques for evaluation of cartilage degeneration in osteoarthritis. *Osteoarthritis Cartilage* 2015;23(10):1639–1653

- 30 Hesper T, Hosalkar HS, Bittersohl D, et al. T2\* mapping for articular cartilage assessment: principles, current applications, and future prospects. *Skeletal Radiol* 2014;43(10):1429–1445
- 31 Aznar MC, Sersar R, Saabye J, et al. Whole-body PET/MRI: the effect of bone attenuation during MR-based attenuation correction in oncology imaging. *Eur J Radiol* 2014;83(07):1177–1183
- 32 Jena A, Taneja S, Rana P, et al. Emerging role of integrated PET-MRI in osteoarthritis. *Skeletal Radiol* 2021;50(12):2349–2363
- 33 Antony B, Singh A. Imaging and biochemical markers for osteoarthritis. *Diagnostics (Basel)* 2021;11(07):1205. Doi: 10.3390/diagnostics11071205